34th Annual International Conference of the IEEE EMBS
San Diego, California USA, 28 August - 1 September, 2012

Effects of Electroconvulsive Therapy Stimulus Pulsewidth and Amplitude Computed with an Anatomically-Realistic Head Model

Siwei Bai, *Student Member*, *IEEE*, Colleen Loo, and Socrates Dokos, *Member*, *IEEE*

***Abstract*— The efficacy and cognitive outcomes of electroconvulsive therapy (ECT) on psychiatric disorders have been shown to depend on variations in treatment technique. In order to investigate this, a high resolution finite element human head model was generated from MRI scans and implemented with tissue heterogeneity and an excitable ionic neural formulations in the brain. The model was used to compare the effects of altered ECT stimulus amplitude and pulse width on the spatial extent of directly activated brain regions. The results showed that decreases in both amplitude and pulse width could effectively lead to reductions in the size of activated brain regions.**

I. Introduction

Electroconvulsive therapy (ECT) is a highly effective procedure for treatment-resistant depression and other severe psychiatric disorders. Contemporary ECT generally involves passing biphasic brief-pulse currents transcranially into a patient under anaesthesia, producing a generalized seizure [1]. Recent clinical research has demonstrated that aside from electrode montage, alteration of stimulus parameters such as pulse width (PW) can also vary the outcome of ECT treatment [2], [3]. Clinical studies using ultrabrief-pulse ECT (PW less than 0.5 ms) reported similar efficacy to brief-pulse ECT (PW in the 0.5-2.0 ms range), with less side effects [2]–[4]. It has been proposed that this may be due to the fact that the volume of directly activated tissue is less with a briefer PW [5]–[7]. Similarly, since the degree of brain activation and inhibition is related to the strength of the local electric field (E-field) [7], [8], a reduced stimulus amplitude in theory may also increase the focality of the therapy. However, modern ECT studies seldom draw attention to the manipulation of pulse amplitude; instead, the amplitude is typically fixed at 800 or 900 mA [7].

Peterchev *et al.* [7] used a sphere model to demonstrate the difference in E-field distributions with various current amplitudes. However, this highly simplified model did not include neural activation by incorporating, for example, excitable neural elements in the brain. We previously proposed a direct brain excitation model by adopting a modified bidomain Hodgkin-Huxley formulation of ion currents, and made a preliminary comparison of the effects of stimulus PW and amplitude [5]. But since the geometry of that head model was derived from downsampled computed tomography (CT) scans, the anatomical structure of the brain was not accurate. As a result, the model could not account for local non-uniformities in current density caused by the complex geometry of the brain and regional differences in tissue conductivity [9], [10]. In addition, the skull was modeled as one homogeneous compartment with anisotropic conductivity which did not accurately represent its three-layered structure.

S. Bai and S. Dokos are with the Graduate School of Biomedical Engineering, Faculty of Engineering, University of New South Wales (UNSW), Sydney, Australia. C. Loo is with the School of Psychiatry, UNSW, Department of Psychiatry, St George Hospital and the Black Dog Institute, Sydney, Australia. Email: s.bai@student.unsw.edu.au; s.dokos@unsw.edu.au; colleen.loo@unsw.edu.au.

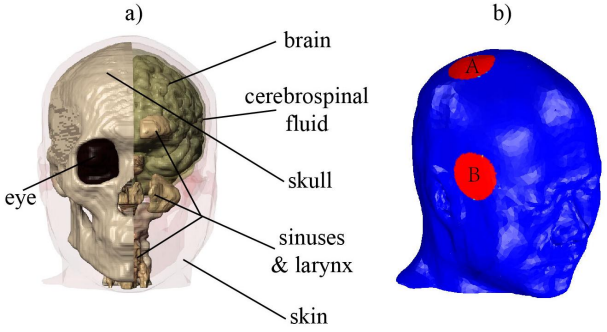

Fig. 1. a: Segmentation of human head: skin, eye, paranasal sinuses (with larynx), skull (including compact bone tissue and spongy bone tissue), vertebrae, cerebrospinal fluid and brain (including grey matter, white matter, cerebellum and spinal cord). b: Right unilateral (RUL) electrode placement. 'A' and 'B' are labels for the separate electrodes used.

In this study, a finite element (FE) model of the human head based on magnetic resonance imaging (MRI) data was utilized to simulate direct brain excitation, including an excitable ionic neural model incorporated in the brain. The objective of the study was to compare the effects of altered ECT stimulus PW and amplitude using this anatomically-realistic head model.

II. Methods

A. Image segmentation and finite element mesh generation

T1-weighted MR images of a healthy 35-year-old male subject were obtained from Neuroscience Research Australia (NeuRA, Sydney). Scan resolution was 1 mm in every direction.

Head tissue masks were initially obtained from the MRI data using BrainSuite2 (www.loni.ucla.edu/Software/BrainSuite) automated mask-generation software. Tissue compartments segmented included the skin, skull, cerebrospinal fluid (CSF), grey matter (GM) and white matter (WM). Mask information was then imported into ScanIP (Simpleware Ltd., UK) for further processing and the tissue masks were subdivided and smoothed. Masks representing eyes, paranasal sinuses,

larynx and cervical vertebrae were separated from skin and skull, as shown in Fig. 1a. The skull was then divided into two compartments including compact bone tissue (with the jaw) and spongy bone tissue. The brain masks were also sectioned into GM, WM, cerebellum (CB, with brainstem) and the cervical spinal cord (SC). Later, to increase computational efficiency, the images were downsampled to a resolution of 1.5 mm in every direction.

The +FE-Free meshing algorithm in ScanIP was chosen to generate the mesh. The resulting mesh model consisted of 1,126,135 elements.

B. White matter conductivity anisotropy

Diffusion tensor (DT) MRI was performed on the same subject in 61 directions. The slices were axially oriented with voxel resolution of 2.5 × 2.5 × 2.5 mm. After registration to the structural scans, the images were imported into FSL (www.fmrib.ox.ac.uk/fsl/index.html) for diffusion tensor calculation, performed using a probabilistic tracking algorithm in the software's FDT diffusion toolbox [11]–[13]. Eigenvectors and fractional anisotropy (FA) were then calculated: the latter being widely used to denote the degree of anisotropy and is typically greater than 0.45 for WM [14].

It was assumed that the electric conductivity tensor shares the same eigenvalues as the water diffusion tensor [15]. Therefore, the conductivity tensor σ for WM was calculated using [16], [17]:

$$\boldsymbol{\sigma} = \mathbf{S}\,\mathrm{diag}(\sigma_l, \sigma_t, \sigma_t)\,\mathbf{S}^T. \tag{1}$$

Only fibre conductivities with strong fractional anisotropy signal (FA $\geq$ 0.45) were calculated.

C. Field solver for volume conductors

Conductivities of the head tissue compartments were taken from Bai *et al.* [17]. ECT electrodes were defined mathematically as circular regions of radius 2.5 cm on the scalp [5]. The electrode configuration used was right unilateral (RUL), *i.e.* one electrode (A) was placed just to the right of the vertex of the head, and the other electrode (B) was placed in the temporal position on the right side of the scalp, as shown in Fig. 1b. Our modeled stimulus current waveforms are shown in Figs. 2a and 3a, where the waveforms are biphasic with anodic-first stimulation applied to electrode A (Fig. 1a). Transcranial stimulation was carried out at 120 Hz, simulating for a total of three periods, *i.e.* 25 ms, plus 1 ms before the first pulse was delivered. The time between anodic onset and cathodic offset was set to half the stimulus period, or 4.17 ms. The effects of variations in stimulus parameters were also investigated, with combinations of parameters listed in Table I. A total of three simulations were undertaken.

Brain compartments including GM, WM and CB were simulated using a modified bidomain ionic continuum model based on the Hodgkin-Huxley formulation [18]. Detailed descriptions of the model can be found in Bai *et al*. [5]. Remaining head compartments were simulated as passive volume conductors. The boundary conditions were:

TABLE I
ECT STIMULUS PARAMETERS

Stimulus Mode	Amplitude (mA)	PW (ms)	Frequency (Hz)	No. of Cycles
control	800	1	120	3
low-amplitude	500	1	120	3
low-PW	800	0.3	120	3

- active electrode boundary: inward current density set to J_n , where

$$J_n = \frac{I(t)}{\text{area of electrode}}, \tag{2}$$

  with $I(t)$ defined as the electrode stimulus current waveform;
- return electrode boundary: inward current density set to $-J_n$;
- distributed resistance boundary (at the bottom of the neck): outward current flow with ground 3 cm distant;
- all other external boundaries treated as electric insulators (zero normal current density);
- continuous current density across all interior boundaries.

The models had more than 6×10^6 degrees of freedom. They were solved in COMSOL Multiphysics (COMSOL AB, Sweden) using a segregated numerical solver on a Windows 64-bit workstation with 24 GB RAM utilizing 4 processors. To solve the time-dependent equations, a variable step backward differentiation formula (BDF) scheme was utilized with an absolute error tolerance set to 10^{-3}. It took approximately 144 hours to solve for a 26-millisecond simulation.

III. RESULTS

Fig. 2b shows the comparison of transmembrane potential (MP) within the activated region in the right temporal lobe between control and low-amplitude current stimuli. Under both situations, the first and the third positive pulses were able to initiate an action potential (AP), whereas the second positive pulse failed to elicit an AP. The initiation of AP in low-amplitude stimulation, however, was slightly slower than that in control.

Fig. 3b compares the MPs at the same site in control and low-PW stimulus modes. Similarly for both cases, only the first and third positive pulses were able to trigger an AP. The initiation of AP in low-PW was delayed relative to that of control. In addition, the depolarization due to the second pulse in low-PW was also much weaker than that of control.

Fig. 4 presents the average MP throughout the stimulus train, which starts from the delivery of the first pulse (t = 1 ms) to the end of the third period (t = 26 ms). Brain regions with average MP $\geq$ -55.59 mV, approximated using MATLAB (The MathWorks Inc., MA) by assuming at least one AP in every two full stimulus cycles, are considered as activated. In the control mode, the stimulus directly activated a large portion of the parietal and right temporal lobes, as

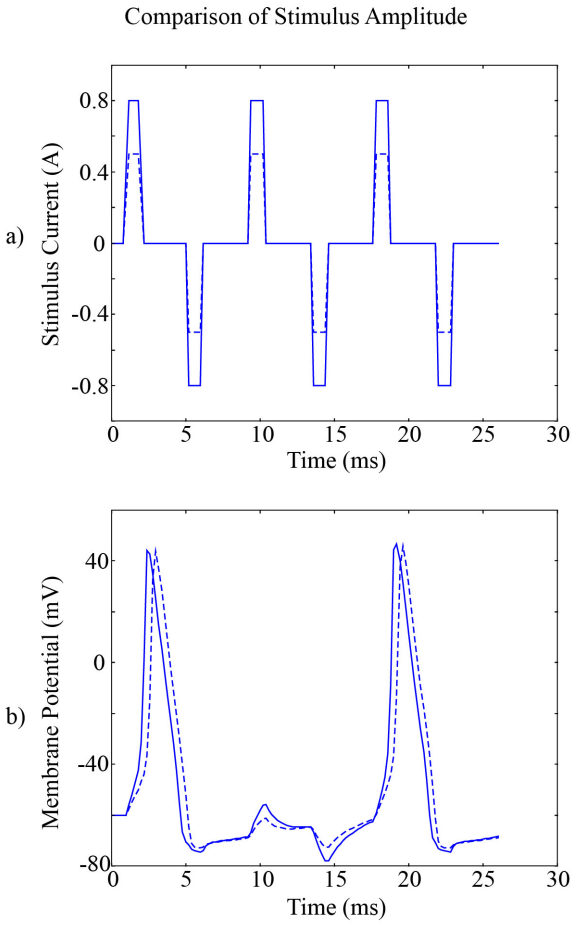

Fig. 2. ECT stimulus waveform (a) and transmembrane potential within activated right temporal region (b, close to cortical surface) in RUL ECT during biphasic stimulation. Each stimulus pulse had an amplitude of 800 mA (solid line) or 500 mA (dashed line). The stimulus was cathodic first with respect to the right temporal lobe electrode B.

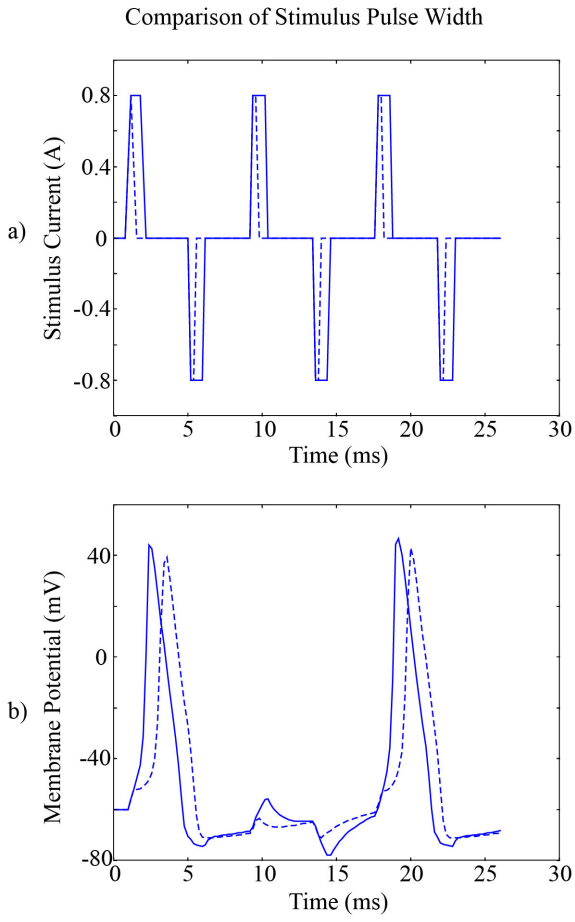

Fig. 3. ECT stimulus waveform (a) and transmembrane potential within activated right temporal region (b, close to cortical surface) in RUL ECT during biphasic stimulation. Each stimulus phase was of pulsewidth 1 ms (solid line) or 0.3 ms (dashed line). The stimulus was cathodic first with respect to the right temporal lobe electrode B.

TABLE II

PERCENTAGE OF BRAIN WITH AVERAGE MP $\geq$ -55.59 MV

Stimulus Mode	Volume (%)	Surface Area (%)
control	26.38	44.78
low-amplitude	12.24	26.87
low-PW	3.33	11.75

well as a portion of the right frontal lobe. In addition, the right part of the cerebellum and the brainstem were also affected. But in low-amplitude and low-PW stimulus modes, the size of directly-activated regions significantly decreased, and the cerebellum and brainstem both showed minimal activation. Table II compares the spatial extent of activated regions in the brain for all three stimulus modes.

IV. DISCUSSION AND CONCLUSION

This study demonstrates the effects of ECT stimulus amplitude and PW on the spatial extent of activated brain regions, using an anatomically-accurate human head model. As a result of evidence that ECT with ultrabrief pulsewidths can reduce cognitive side effects while maintaining useful efficacy [2]–[4], [19], it has been suggested that due to less energy and charge transfer in briefer pulses, a narrower band of tissue may be stimulated, minimizing the activation of non-targeted brain tissue [6], [7]. In a previous study, we investigated the likelihood of this hypothesis using a down-sampled model [5]. In this present study, using an anatomically-accurate model with three-layered skull and anisotropic white matter conductivity, we have now confirmed these findings.

The data of Table II indicates that in both the low-amplitude and low-PW stimulus modes, the volume of directly-activated regions is lowered more than their surface area. This suggests that the decrease in PW (or amplitude) exerts most influence on deeper brain regions (such as the hippocampus), which may explain the reduction in cognitive side effects during ultrabrief stimulation. Further studies are needed to investigate this model prediction.

The reason why stimulus in the second cycle were unable to trigger APs is that the neurons were still in their refractory state when the pulses were delivered. The refractory period

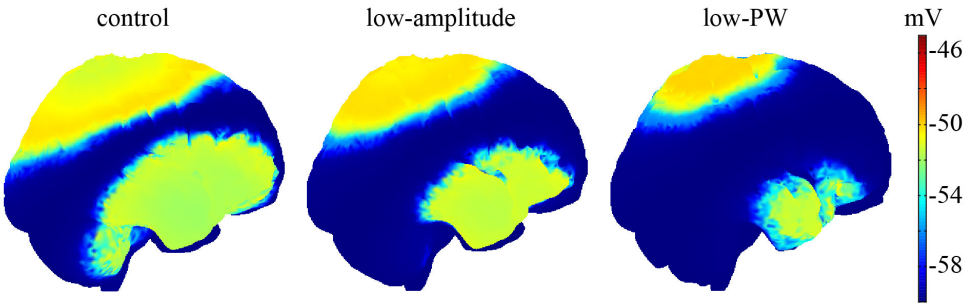

Fig. 4. Average membrane potential throughout the stimulus train, beginning from the delivery of the first pulse to the end of the third cycle, under the three stimulus modes.

for neurons is typically around 3 ms [20], and for some neurons it can last longer than 5 ms [21]. During the refractory period, the AP is either unable to be initiated, or requires much higher stimulus energy to be initiated. Therefore, only a slight depolarization (and hyperpolarization) can be seen after the delivery of the stimuli in the second cycle (Figs 2b and 3b). Previous studies have shown that ECT with low frequencies is more efficient than high frequencies in inducing seizure [7]. This may be due to the fact that stimuli with lower frequencies are able to initiate more APs efficiently than higher frequencies, accounting for improved seizure-induction ability. Since clinical ECT conventionally employs 30-120 Hz, further investigations are needed to test this finding over a range of frequencies.

V. Acknowledgment

The authors would like to thank Prof. Caroline Rae and Dr. John Geng from Neuroscience Research Australia for their support in acquiring and processing the structural MRI and DT-MRI data, and Dr. Elizabeth Tancred from the University of New South Wales for her assistance with the head anatomy.

References

[1] R. Abrams, *Electroconvulsive therapy*. New York: Oxford University Press, 2002.

[2] C. Loo, K. Sainsbury, P. Sheehan, and B. Lyndon, "A comparison of RUL ultrabrief pulse (0.3 ms) ECT and standard RUL ECT," *Int J Neuropsychopharmacol*, vol. 11, no. 7, pp. 883–890, 2008.

[3] H. Sackeim, J. Prudic, M. Nobler, L. Fitzsimons, S. Lisanby, N. Payne, R. Berman, E. Brakemeier, T. Perera, and D. Devanand, "Effects of pulse width and electrode placement on the efficacy and cognitive effects of electroconvulsive therapy," *Brain Stimulat*, vol. 1, no. 2, pp. 71–83, 2008.

[4] P. Sienaert, K. Vansteelandt, K. Demyttenaere, and J. Peuskens, "Randomized comparison of ultra-brief bifrontal and unilateral electroconvulsive therapy for major depression: Clinical efficacy," *J Affect Disord*, vol. 116, no. 1-2, pp. 106–112, 2009.

[5] S. Bai, C. Loo, A. Al Abed, and S. Dokos, "A computational model of direct brain excitation induced by electroconvulsive therapy: Comparison among three conventional electrode placements," *Brain Stimulat*, vol. doi:10.1016/j.brs.2011.07.004, 2011.

[6] H. Sackeim, "Convulsant and anticonvulsant properties of electroconvulsive therapy: Towards a focal form of brain stimulation," *Clin Neurosci Res*, vol. 4, no. 1-2, pp. 39–57, 2004.

[7] A. Peterchev, M. Rosa, Z. Deng, J. Prudic, and S. Lisanby, "Electroconvulsive therapy stimulus parameters: Rethinking dosage," *J ECT*, vol. 26, no. 3, pp. 159–174, 2010.

[8] T. Wagner, A. Valero-Cabre, and A. Pascual-Leone, "Noninvasive human brain stimulation," *Annu Rev Biomed Eng*, vol. 9, pp. 527–565, 2007.

[9] A. Datta, V. Bansal, J. Diaz, J. Patel, D. Reato, and M. Bikson, "Gyri-precise head model of transcranial direct current stimulation: Improved spatial focality using a ring electrode versus conventional rectangular pad," *Brain Stimulat*, vol. 2, no. 4, pp. 201–207, 2009.

[10] R. Salvador, A. Mekonnen, G. Ruffini, and P. Miranda, "Modeling the electric field induced in a high resolution realistic head model during transcranial current stimulation," in *Conf Proc IEEE Eng Med Biol Soc, 2010*, 2010, pp. 2073–2076.

[11] T. Behrens, M. Woolrich, M. Jenkinson, H. Johansen-Berg, R. Nunes, S. Clare, P. Matthews, J. Brady, and S. Smith, "Characterization and propagation of uncertainty in diffusion-weighted MR imaging," *Magn Reson Med*, vol. 50, no. 5, pp. 1077–1088, 2003.

[12] T. Behrens, H. Johansen-Berg, M. Woolrich, S. Smith, C. Wheeler-Kingshott, P. Boulby, G. Barker, E. Sillery, K. Sheehan, O. Ciccarelli, A. Thompson, J. Brady, and P. Matthews, "Non-invasive mapping of connections between human thalamus and cortex using diffusion imaging," *Nat Neurosci*, vol. 6, no. 7, pp. 750–757, 2003.

[13] T. Behrens, H. Berg, S. Jbabdi, M. Rushworth, and M. Woolrich, "Probabilistic diffusion tractography with multiple fibre orientations: What can we gain?" *Neuroimage*, vol. 34, no. 1, pp. 144–155, 2007.

[14] H. Johansen-Berg and T. Behrens, *Diffusion MRI: From quantitative measurement to in-vivo neuroanatomy*. London: Academic Press, 2009.

[15] P. Basser, J. Mattiello, and D. LeBihan, "MR diffusion tensor spectroscopy and imaging," *Biophys J*, vol. 66, no. 1, pp. 259–267, 1994.

[16] C. Wolters, A. Anwander, X. Tricoche, D. Weinstein, M. Koch, and R. MacLeod, "Influence of tissue conductivity anisotropy on EEG/MEG field and return current computation in a realistic head model: A simulation and visualization study using high-resolution finite element modeling," *Neuroimage*, vol. 30, no. 3, pp. 813–826, 2006.

[17] S. Bai, C. Loo, G. Geng, and S. Dokos, "Effect of white matter anisotropy in modeling electroconvulsive therapy," in *Conf Proc IEEE Eng Med Biol Soc, 2011*, 2011, pp. 5492–5495.

[18] A. Hodgkin and A. Huxley, "A quantitative description of membrane current and its application to conduction and excitation in nerve," *J Physiol*, vol. 117, no. 4, pp. 500–544, 1952.

[19] C. Loo, P. Sheehan, M. Pigot, and W. Lyndon, "A report on mood and cognitive outcomes with right unilateral ultrabrief pulsewidth (0.3 ms) ECT and retrospective comparison with standard pulsewidth right unilateral ECT," *J Affect Disord*, vol. 103, no. 1-3, pp. 277–281, 2007.

[20] J. Nolte, *The human brain: An introduction to its functional anatomy, 6th ed.* Philadelphia: Mosby, Elsevier, 2009.

[21] T. Nick and A. Ribera, "Synaptic activity modulates presynaptic excitability," *Nat Neurosci*, vol. 3, pp. 142–149, 2000.